

Sirt1 induction confers resistance to etoposide-induced genotoxic apoptosis in thyroid cancers

KI HWAN KWEON^{1,3*}, CHO ROK LEE^{1*}, SOO JUNG JUNG¹, EUN JEONG BAN¹, SANG-WOOK KANG¹, JONG JU JEONG¹, KEE-HYUN NAM¹, YOUNG SUK JO², JANDEE LEE¹ and WOONG YOUN CHUNG¹

Departments of ¹Surgery and ²Internal Medicine, Severance Hospital, Yonsei Cancer Center, Yonsei University College of Medicine, Seoul 120-752; ³Department of Surgery, Hongik Hospital, Yangcheon-gu, Seoul, Republic of Korea

Received June 11, 2014; Accepted July 18, 2014

DOI: 10.3892/ijo.2014.2585

Abstract. Despite the favorable therapeutic outcomes reported in differentiated thyroid cancer (DTC), a significant proportion of DTC patients present with refractory behavior to conventional therapy. The sirtuin (Sirt) family has recently been implicated in the maintenance of cellular homeostasis under genotoxic stress. Here, we investigated the induction of Sirt1 expression by etoposide-induced genotoxic stress to gain insights into thyroid carcinogenesis and identify novel therapeutic targets. Immunohistochemical staining analyses of Sirt1 and Sirt3 were performed using human thyroid cancer tissues and matched normal tissues, and bioinformatic analyses were done using public repositories, including the Human Protein Atlas, BioGPS, NCBI Gene Expression Omnibus (GEO) profiles, and GeneNetwork. TPC1, FTC133 and FRO cells were used for molecular biological experiments including apoptosis assays, MTT, immunofluorescence staining and qRT-PCR assays. The IHC data and public repositories data consistently showed variable Sirt1 and Sirt3 expression patterns in normal thyroid follicular cells and papillary thyroid cancer cells. The induction of Sirt1 and Sirt3 was cell type-specific and the expression levels of these genes correlated with apoptotic cell death and cell viability after etoposide-induced genotoxic stress. Sirt1-Foxp3 signaling-mediated regulation of Bax and p21 mRNA expression was a signature molecular event in TPC1 cells, which showed remarkable resistance to etoposide-induced genotoxic stress. The induction of Sirt1 and Sirt3 may be a determinant of thyroid cancer cell survival under genotoxic stress conditions. Further examination of the

Sirt1-Foxp3 signal may improve our understanding of thyroid carcinogenesis and help identify new druggable targets.

Introduction

Thyroid cancer is the most common cancer of the endocrine system. In the United States, differentiated thyroid cancer (DTC) is the sixth most common cancer among women and the eight most common cancer overall (<http://seer.cancer.gov/statfacts/html/thyro.html>). Most DTCs respond favorably to conventional therapy such as thyroidectomy and radioactive iodine (RAI) therapy. However, a significant proportion of patients with DTC develop life-threatening RAI-refractory disease that is usually resistant to cytotoxic chemotherapy (1-4). Because of this poor response to cytotoxic chemotherapy, new molecular-targeted therapies are being developed for the treatment of DTC patients who require systemic therapy (3,5). In this context, protein kinase inhibitors targeting the RAS-RAF-MEK-ERK (MAPK) signaling pathway have been investigated intensively and BRAF inhibitors have shown beneficial effects in clinical trials (6-8). However, the development of resistance to kinase inhibitors is an emerging problem for clinicians and patients, and the design of strategies to overcome this resistance is a primary concern of researchers (9,10).

Mammalian sirtuin 1 (Sirt1) belongs to a highly conserved family of nicotinamide adenosine dinucleotide-dependent (NAD⁺-dependent) protein deacetylases and is widely expressed in most mammalian organs (11). The deacetylase activity of Sirt1 and its role in the regulation of several stress-induced transcription factors such as p53, heat shock transcription factor 1 (HSF1), nuclear factor κ B (NF- κ B), peroxisome proliferator-activated receptor γ , coactivator 1 α (PGC-1 α) and the forkhead box O (FOXO) family of transcription factors have been studied extensively (12-16). The activation of Sirt1 in response to stress may therefore be an evolutionarily conserved process to drive cellular homeostasis related to oxidative stress and apoptosis (17). Sirt1 activity is modulated by calorie restriction (CR), HuR, NAD⁺ and active regulator of Sirt1 (AROS); in turn, the deacetylase activity of Sirt1 promotes stress adaptation responses including DNA repair and anti-apoptotic effects in response to genotoxic stress (18-23). However, its dynamic role in the regulation of

Correspondence to: Dr Jandee Lee, Department of Surgery, Severance Hospital, Yonsei Cancer Center, Yonsei University College of Medicine, Seoul 120-752, Republic of Korea
E-mail: jandee@yuhs.ac

*Contributed equally

Key words: thyroid neoplasm, Sirtuin 1, drug resistance, apoptosis, DNA damage

cytoprotective effects and apoptosis suggests that Sirt1 acts both as an oncogene and a tumor suppressor (24,25).

In the present study, we investigated the cytoprotective effects of Sirt1 in thyroid cancer cells exposed to genotoxic stress induced by etoposide treatment, which can cause DNA damage by preventing the re-ligation of DNA strands and promoting DNA strand breaks (26). Our results showed that the etoposide-induced differential expression of Sirt1 is cell type-specific and related to the resistance of thyroid cancer cells to etoposide-induced cell death. Our data also indicated that Bax and p21 are signature molecules possibly associated with the cytoprotective effects of Sirt1.

Materials and methods

Tissue specimens and immunohistochemical analysis. Thyroid tissue specimens were obtained from 50 patients with papillary thyroid cancer (PTC) who underwent surgery from 2010 to 2013 at the Yonsei Cancer Center, Yonsei University College of Medicine (Seoul, Korea). All protocols were approved by the institutional review board and written informed consent was obtained from all subjects. Immunohistochemical (IHC) staining for Sirt1 and Sirt3 was performed in PTC samples and matched normal tissues. Tissue sections were incubated with primary antibodies against Sirt1 (sc-15404, Santa Cruz Biotechnology, Santa Cruz, CA, USA) and Sirt3 (sc-99143, Santa Cruz Biotechnology).

Cell lines and materials. TPC-1 (papillary thyroid cancer cell line) and FTC-133 (follicular thyroid cancer cell line) cells were cultured in DMEM (Sigma, St. Louis, MO, USA) supplemented with 10% FBS. FRO (undifferentiated/anaplastic thyroid cancer cell line) cells were cultured in RPMI-1640 (Sigma) with 10% FBS. Etoposide (Sigma) was used at 20 μ M for the indicated times.

Immunoblot analysis. Cells were lysed in lysis buffer, and cell lysates were separated using SDS-polyacrylamide gel electrophoresis. Proteins were transferred to nitrocellulose (NS) membranes (Amersham Biosciences, Freiburg, Germany), which were blocked with 5% skim milk and incubated with the indicated primary antibodies overnight at 4°C. After washing, the membranes were incubated with secondary antibodies for 1 h at room temperature. The immunoreactive bands were visualized using peroxidase-conjugated secondary antibodies (Phototope-HRP Western Blot Detection Kit, New England Biolabs, Beverly, MA, USA). The primary antibodies used in this study were obtained from Santa Cruz Biotechnology (Santa Cruz, CA, USA) and were as follows: anti-Sirt1 (sc-15404), anti-Sirt3 (sc-365175), and anti-actin (sc-1616).

Immunofluorescence staining. Cells were plated at 1×10^5 cells/well on coverslips in 6-well plates. After 3 days, cells were fixed and permeabilized using conventional methods. Then, the cells were incubated with anti-Sirt1 (sc-15404, Santa Cruz Biotechnology) and anti-p21 (sc-397, Santa Cruz Biotechnology) antibodies at a 1:100 dilution in 3% bovine serum albumin for 24 h at 4°C. After washing, cells were incubated with goat anti-rabbit IgG H&L (Alexa Fluor® 488) (ab150077, Cambridge, MA, USA). After washing, the cells on

the coverslips were mounted on glass slides using mounting medium (Sigma-Aldrich) and observed using a laser-scanning confocal microscope (Carl Zeiss AG, Oberkochen, Germany). All experiments were performed in triplicate and were repeated at least three times.

Apoptosis detection. Apoptosis was assessed using the PE Annexin V Apoptosis Detection Kit I (BD Biosciences, Warsaw, Poland) according to the manufacturer's protocol. Briefly, cells were washed twice with cold PBS and re-suspended in 1X binding buffer at a concentration of 1×10^6 cells/ml. Then, 100 μ l of the solution (1×10^5 cells) was transferred to a 5-ml culture tube, treated with 5 μ l of FITC Annexin V and 5 μ l of propidium iodide (PI), and incubated for 15 min at RT (25°C) in the dark. After adding 400 μ l of 1X binding buffer to each tube, flow cytometry analysis was performed. Data were analyzed using a BD FACSVerser system and BD FACSuite software (BD Biosciences).

MTT (3-[4,5-dimethylthiazol-2-yl]-2,5-diphenyltetrazolium bromide) assay. Cell viability was assessed by the MTT dye conversion assay. After treatment with etoposide, MTT (25 μ l of 5 mg/ml MTT in sterile PBS) was added to 100 μ l of a cell suspension and incubated for 2 h at 37°C. After the reaction was stopped, the cells were lysed by addition of 100 μ l lysis buffer. Cell lysates were incubated at 37°C overnight to allow cell lysis and dye solubilization. The OD was read at 595 nm using a THERMOMax microplate reader (Molecular Devices, Menlo Park, CA, USA). Data are expressed as a percentage of vehicle-treated (DMSO) control values and are the result of three independent experiments, each performed in triplicate.

RNA isolation and real-time PCR. Total RNA was extracted using TRIzol (Invitrogen, Carlsbad, CA, USA) and complementary DNA (cDNA) was prepared from total RNA using M-MLV Reverse Transcriptase (Invitrogen) and oligo-dT primers (Promega, Madison, WI, USA). Quantitative RT-PCR (qRT-PCR) was performed using cDNA, a QuantiTect SYBR® Green RT-PCR kits (Qiagen, Valencia, CA, USA), and the following primers: Bax, 5'-CCC GAG AGG TCT TTT TCC GAG-3' and 5'-CCA GCC CAT GAT GGT TCT GAT-3'; Bcl-xL, 5'-GAG CTG GTG GTT GAC TTT CTC-3' and 5'-TCC ATC TCC GAT TCA GTC CCT-3'; p53, 5'-CAG CAC ATG ACG GAG GTT GT-3' and 5'-TCA TCC AAA TAC TCC ACA CGC-3'; p21, 5'-TGT CCG TCA GAA CCC ATG C-3' and 5'-AAA GTC GAA GTT CCA TCG CTC-3'; and GAPDH, 5'-GGA GCG AGA TCC CTC CAA AAT-3' and 5'-GGC TGT TGT CAT ACT TCT CAT GG-3'. Relative expression was measured using the Applied Biosystems® StepOne™ Real-Time PCR system (Foster City, CA, USA). qRT-PCR experiments were performed in triplicate and repeated three times.

Public data and statistical analysis. Analysis of gene expression using public repository data was performed using the Human Protein Atlas (<http://www.proteinatlas.org/>), BioGPS (<http://biogps.org/#goto=welcome>), NCBI Gene Expression Omnibus (GEO) profiles (<http://www.ncbi.nlm.nih.gov/geo/profiles>), and GeneNetwork (a free scientific web resource, <http://www.genenetwork.org/>). Statistical analysis was performed using GraphPad Prism (GraphPad Software, Inc., CA, USA).

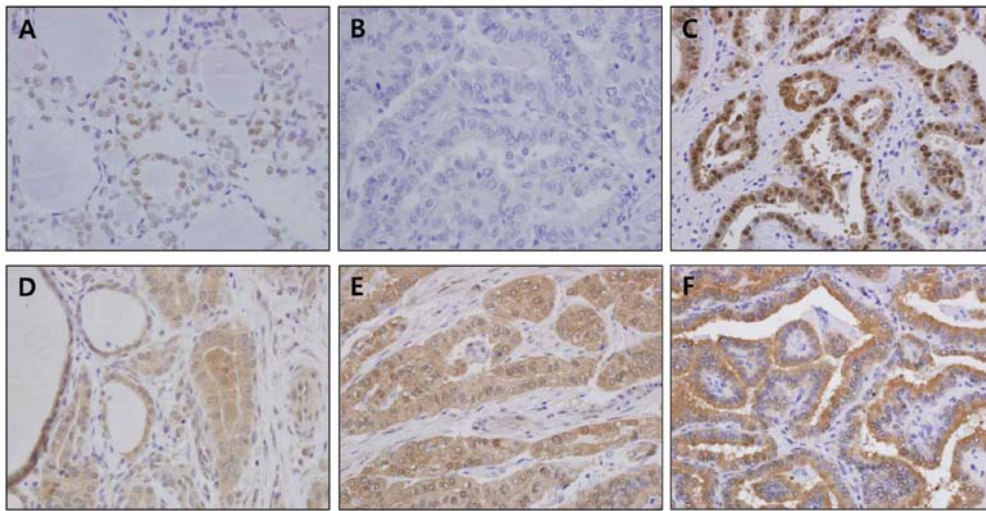


Figure 1. Representative images of immunohistochemical stained normal and papillary thyroid cancer tissues. (A) Sirt1 expression in normal thyroid tissues. (B and C) Sirt1 expression in papillary thyroid cancer tissues. (D) Sirt3 expression in normal and papillary thyroid cancer tissues. (E and F) Sirt3 expression in papillary thyroid cancer tissues. IHC staining was performed using 50 PTC and matched normal tissues.

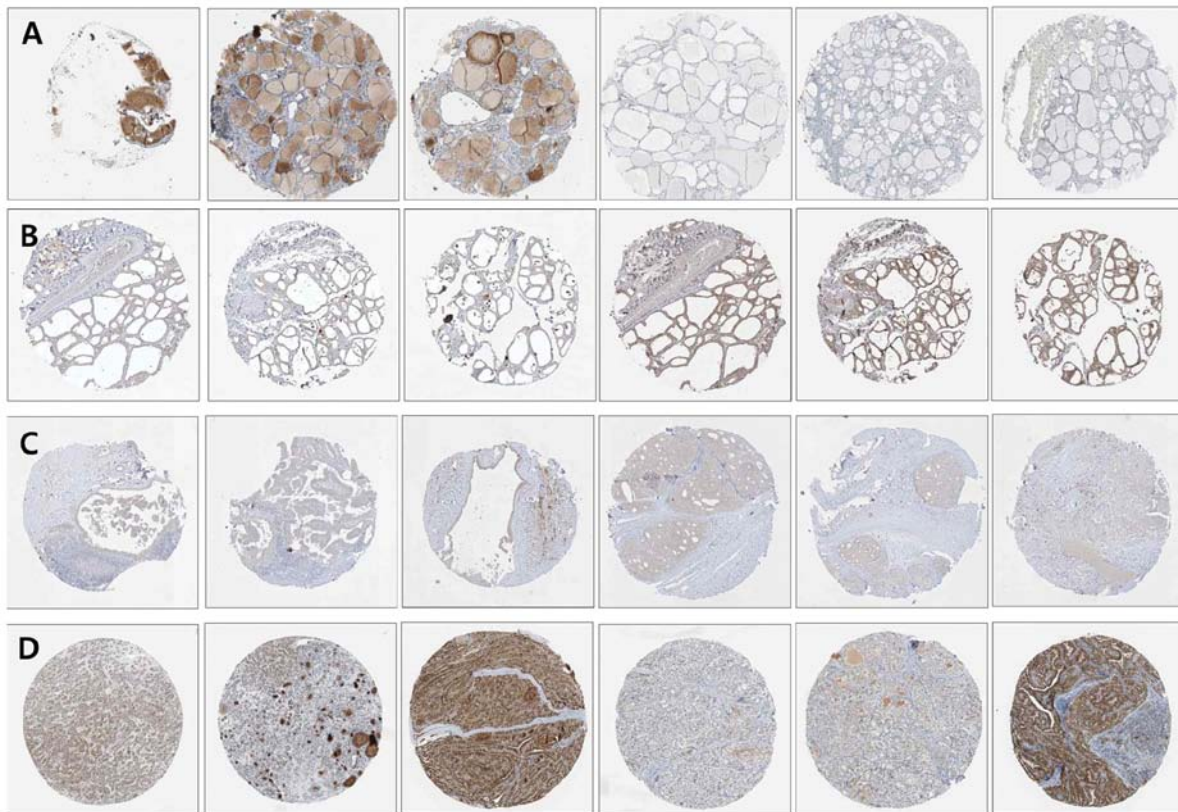


Figure 2. Representative microscopic images of Sirt1 (A and B) and Sirt3 (C and D) expression detected by immunohistochemical staining in normal thyroid follicular cells (A and C) and papillary thyroid cancers (B and D). Data were obtained from the Human Protein Atlas (<http://www.proteinatlas.org/>).

Comparisons were performed with the Mann-Whitney U test. Data are expressed as the mean \pm SEM, * $p < 0.05$, ** $p < 0.01$, *** $p < 0.001$. All reported p -values are two-sided.

Results

Sirt1 is differentially expressed in human papillary thyroid carcinoma. To compare the expression patterns of Sirt1 in

normal and thyroid cancer tissues, we performed IHC using anti-Sirt1 and anti-Sirt3 antibodies. As shown in Fig. 1A, Sirt1 expression in the nuclei of normal follicular cells was variable. In the PTC samples, Sirt1 expression was also variable, and expression ranged from no staining (Fig. 1B) to strong nuclear staining (Fig. 1C). In the case of Sirt3, variable expression levels were observed in normal and PTC tissues (Fig. 1D-F). To support these results, we conducted a search of

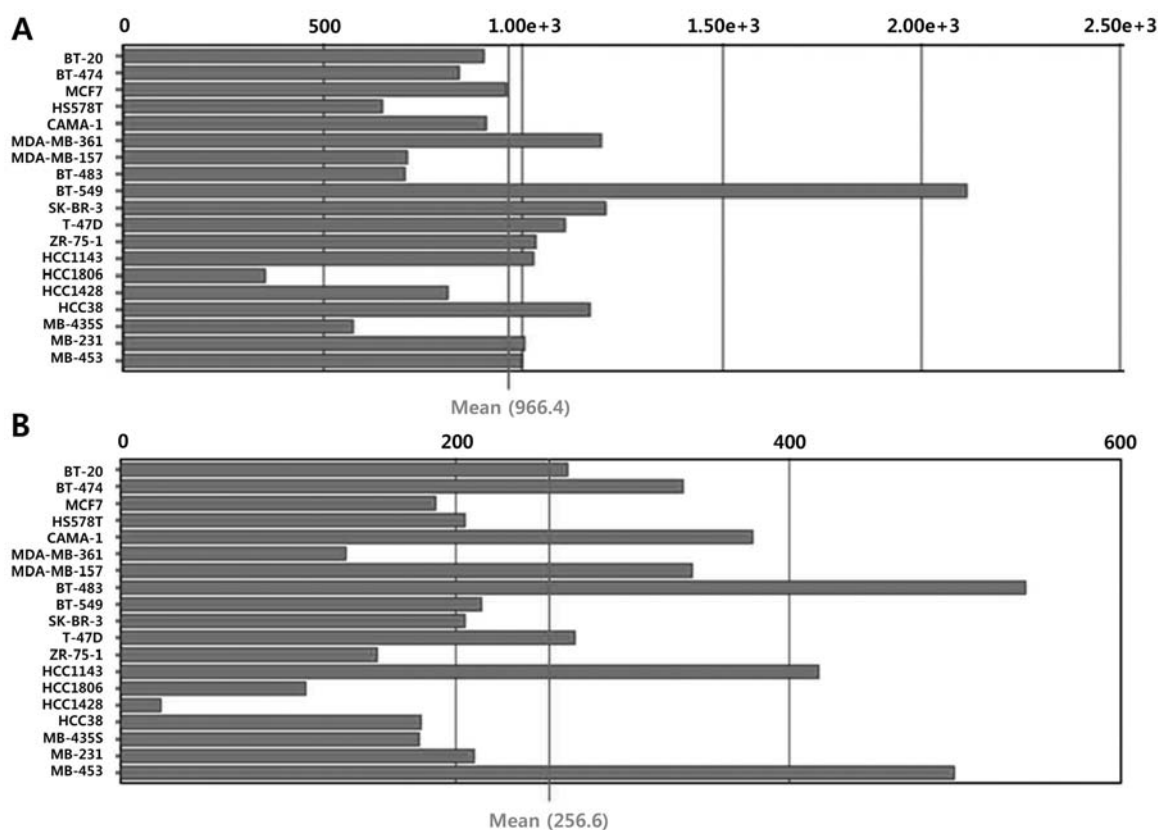


Figure 3. mRNA expression of Sirt1 (A) and Sirt3 (B) in human breast cancer cell lines. Data were obtained from BioGPS (<http://biogps.org/#goto=welcome>).

public gene expression repositories such as the Human Protein Atlas (<http://www.proteinatlas.org/>), BioGPS (<http://biogps.org/#goto=welcome>) and NCBI Gene Expression Omnibus (GEO) profiles (<http://www.ncbi.nlm.nih.gov/geo/profiles>). The Human Protein Atlas showed heterogeneous expression patterns of Sirt1 in normal thyroid and papillary thyroid cancer tissues with remarkable variation from faint to strong expression (Fig. 2A and B). Consistent with the pattern of Sirt1 expression, Sirt3 showed heterogeneous and remarkably variable expression in normal and papillary thyroid cancers tissues (Fig. 2C and D). Because stress-induced changes in Sirt1 levels are regulated not only at the transcriptional level but also by modulation of RNA stability and post-translational control, the mRNA expression levels of Sirt1 and Sirt3 were assessed using BioGPS and NCBI GEO profiles. No data on the mRNA expression profiles of Sirt1 and Sirt3 in thyroid cancers were found in BioGPS; however, variable mRNA expression of Sirt1 and Sirt3 was observed in breast cancer cell lines (Fig. 3). In line with the BioGPS profiles, we consistently found variable Sirt1 and Sirt3 mRNA expression profiles in normal thyroid follicular cells and papillary thyroid cancer cells in the NCBI GEO profiles (Fig. 4). Taken together, our analysis using public repositories indicated that Sirt1 and Sirt3 mRNA and protein expression may be regulated in a cell type- or context-dependent manner.

The induction of Sirt1 expression by etoposide occurs in a cell type-specific manner in thyroid cancer cell lines. Based on the variable expression of Sirt1 and Sirt3 in papillary thyroid cancer, we examined whether etoposide-induced genotoxic

stress has a differential effect on the expression of Sirt1 and Sirt3 in a cell type-specific manner. As shown in Fig. 5A and B, TPC1 cells treated with etoposide (20 μ M) for 24 or 48 h showed increased expression of Sirt1 and Sirt3. However, Sirt1 and Sirt3 were downregulated in FTC133 and FRO cells under the same experimental conditions (Fig. 5C and D). Consistent with our data, a strong positive correlation between Sirt1 and Sirt3 mRNA expression was observed in the GSE16780 UCLA Hybrid MDP Liver Affy HT M430A (Sep11) RMA Database from GeneNetwork (<http://www.genenetwork.org/>) (Fig. 6, Spearman's rank correlation: $Rho=0.496$, $p=3.38 \times 10^{-3}$; Pearson's correlation: $Rho=0.442$, $p=1.06 \times 10^{-2}$). In fact, Sirt3 possesses stress responsive deacetylase activity similar to that of Sirt1, protecting cells from genotoxic and oxidative stress-mediated cell death. Combined with data from the public repository, the differential induction of Sirt1 and Sirt3 in TPC1, FTC133 and FRO cells confirmed that Sirt1 and Sirt3 might function cooperatively in a cell type- or context-dependent manner.

Sirt1 induction is related to etoposide-induced cell death. To support our results suggesting the cell type- or context-dependent action of Sirt1 and Sirt3, we analyzed apoptotic cell death induced by etoposide in TPC1, FTC133 and FRO cells using Annexin V flow cytometric analysis. As shown in Fig. 7A, TPC1 cells showed a minimal increase of apoptosis (5.06%) in response to etoposide (20 μ M) treatment for 48 h compared to the untreated controls (1.9%), whereas 24-h etoposide treatment had no significant effect on the rate of apoptosis (Fig. 7B). By contrast, a dramatic increase of apoptotic cell

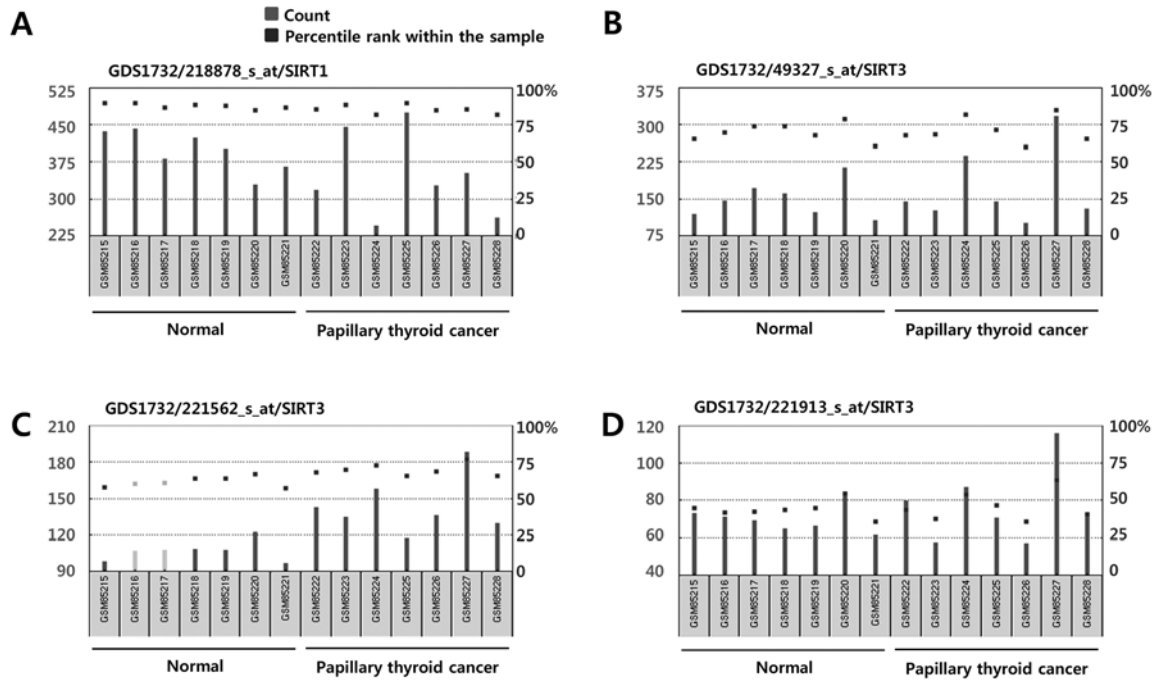


Figure 4. mRNA expression of Sirt1 (A) and Sirt3 (B-D) in human thyroid follicular cells and papillary thyroid cancer cells. Data were obtained from NCBI Gene Expression Omnibus (GEO) profiles (<http://www.ncbi.nlm.nih.gov/geo/profiles>). (A) Sirt1, Reporter: GPL570, 218878_s_at (ID_REF), GDS1732, 23411 (Gene ID), NM_012238. (B) Sirt3, Reporter: GPL570, 49327_at (ID_REF), GDS1732, 23410 (Gene ID), AI492888. (C) Sirt3, Reporter: GPL570, 221562_s_at (ID_REF), GDS1732, 23410 (Gene ID), AF083108. (D) Sirt3, Reporter: GPL570, 221913_at (ID_REF), GDS1732, 23410 (Gene ID), AI492888.

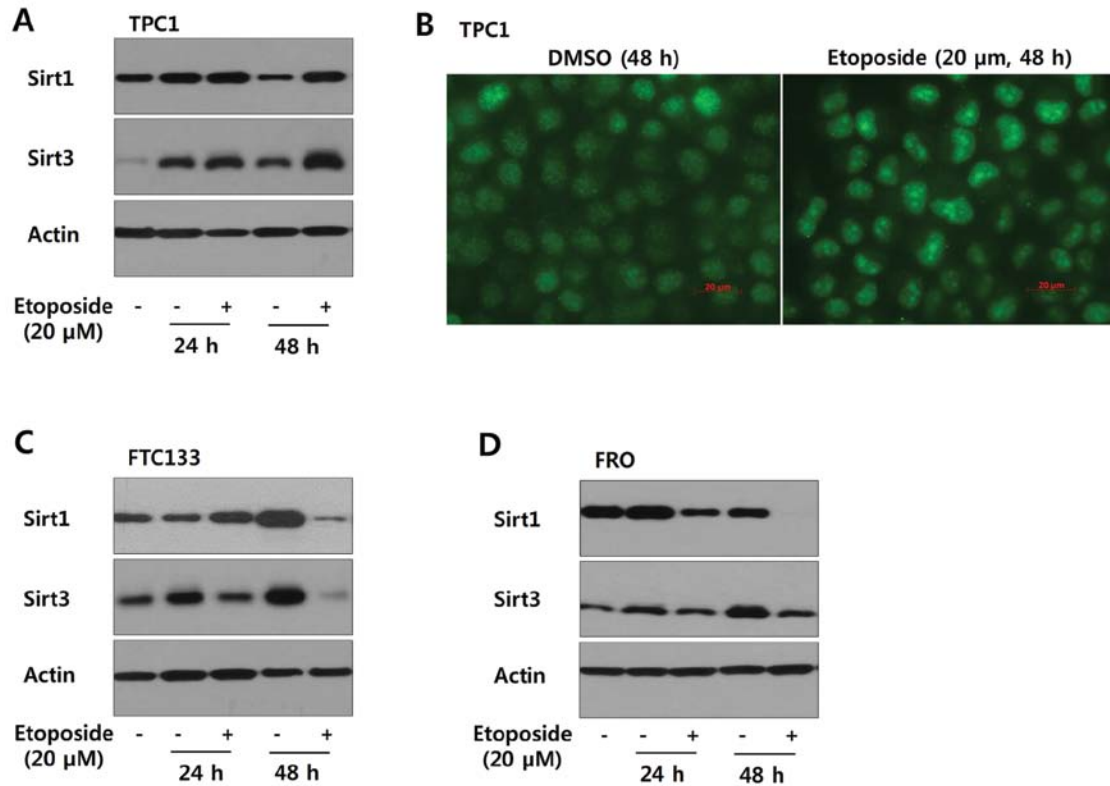


Figure 5. Immunoblot analysis and immunofluorescence staining to detect Sirt1 or Sirt3 after exposure to etoposide for the indicated times in TPC1 (A and B), FTC133 (C) and FRO (D). All data are the result of three independent experiments.

death (58.6%) was observed in response to etoposide for 48 h in FTC133 cells compared to the untreated controls (1.74%, Fig. 7C), and the effect was statistically significant after 24 h

of treatment (Fig. 7D). FRO cells also showed a dramatic increase of apoptotic cell death (1.70 vs. 24.52%) after 48 h of etoposide treatment (Fig. 7E), and this effect was statisti-

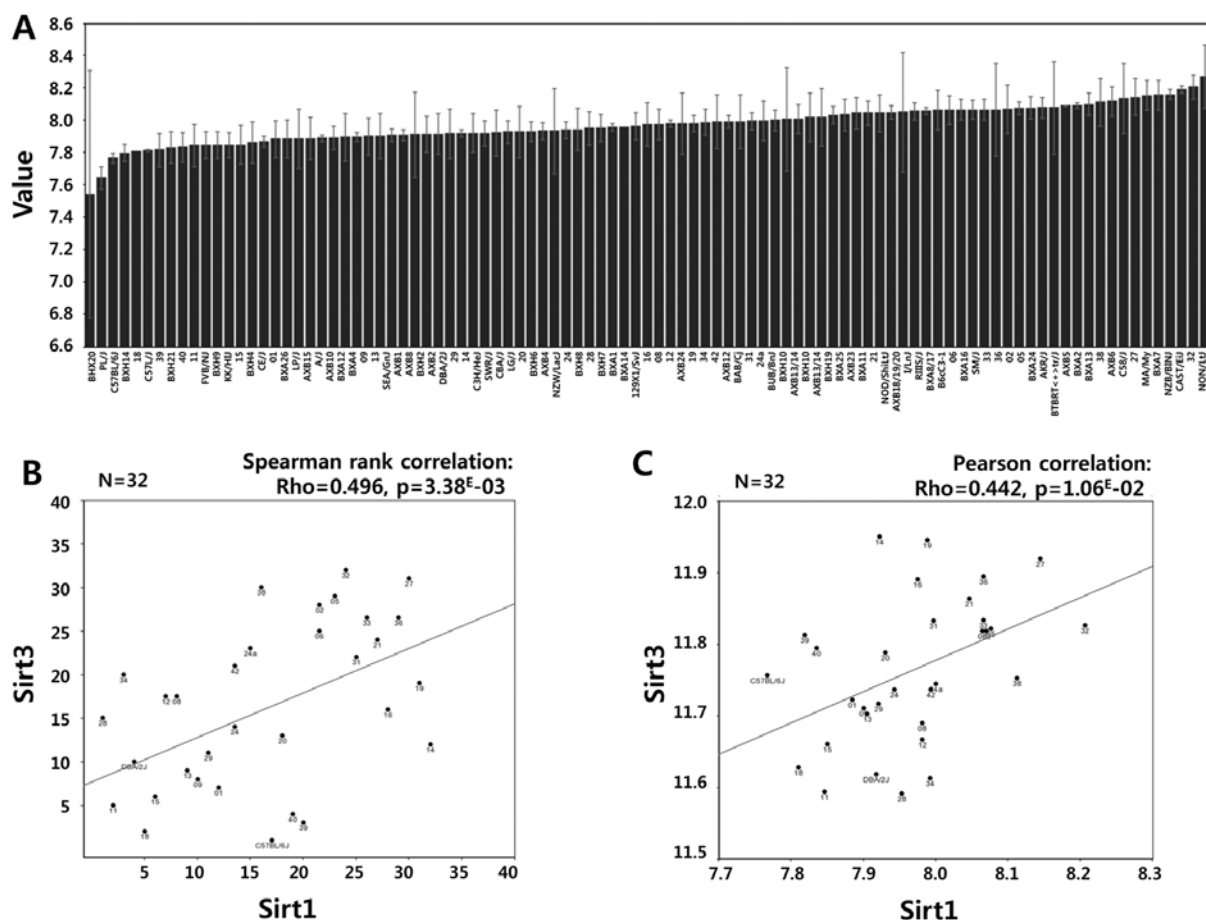


Figure 6. Correlation analysis between Sirt1 and Sirt3 in the GSE16780 UCLA Hybrid MDP Liver Affy HT M430A (Sep11) RMA Database using GeneNetwork (<http://www.genenetwork.org/>). (A) Ranked bar graph showing the number of samples and Sirt1 expression values in each mouse. (B) Spearman's rank correlation: $Rho=0.496$, $p=3.38E-03$. (C) Pearson's correlation: $Rho=0.442$, $p=1.06E-02$.

cally significant after 24 h of treatment (Fig. 7F). To verify the flow cytometry results, cell viability was assessed by MTT assay after exposure to etoposide ($20 \mu\text{M}$) for the indicated times. Consistent with the flow cytometry data, the reduction of enzymatic activity of NAD(P)H-dependent cellular oxidoreductase was lower in TPC1 cells than in FTC133 and FRO cells (Fig. 8A). Taken together, these results suggest that the higher induction of Sirt1 and Sirt3 in TPC1 cells may confer increased resistance against etoposide-induced genotoxic stress, as observed by reduced apoptosis and increased cell viability compared to cells with low Sirt1 and Sirt3 induction.

cDNA microarray data using BXD mice show a correlation of Bax and p21 with Sirt1 activation. To gain insight into the molecular mechanisms via which Sirt1 and Sirt3 contribute to resistance against etoposide-induced genotoxic stress, we reviewed the literature and analyzed public gene expression repositories. A recent study suggested that Sirt1 deacetylates and negatively regulates the forkhead box protein P3 (Foxp3) transcription factor (27). In addition, Ex-527, a Sirt1 inhibitor, enhanced Foxp3 expression during *ex vivo* Treg expansion (27). In line with this recent report, we investigated the correlations between Foxp3 expression and apoptosis-related molecules on GeneNetwork. Interestingly, we found that the mRNA expression of Foxp3 showed a positive relationship

with Bax in the GSE16780 UCLA Hybrid MDP Liver Affy HT M430A (Sep11) RMA Database (Fig. 8, Spearman's rank correlation: $Rho=0.420$, $p=1.60E-02$; Pearson's correlation: $Rho=0.453$, $p=8.49E-03$), suggesting that a Sirt1-Foxp3-Bax signaling pathway contributes to resistance to etoposide-induced genotoxic stress by decreasing Bax expression. In addition, a statistically significant negative correlation between Foxp3 and p21 [cyclin-dependent kinase inhibitor 1A (CDKN1A), Cip1] was also found in EPFL/LISP BXD CD Brown Adipose Affy Mouse Gene 2.0 ST Exon Level (Oct13) RMA (Fig. 9, Spearman's rank correlation: $Rho=-0.471$, $p=2.89E-03$; Pearson's correlation: $Rho=-0.489$, $p=1.82E-03$). Taken together, these results suggest that Sirt1-Foxp3-Bax/p21 signaling might generate a cytoprotective effect in TPC1 cells exposed to etoposide treatment.

The differential expression of Bcl-2 family proteins in TPC1 cells is correlated with Sirt1. To gather further evidence in support of the proposed mechanism of resistance to etoposide in TPC1 cells, we performed qRT-PCR for Bax and p21. In addition, we also included another Bcl-2 family protein, Bcl-xL, and p53, which is the first known non-histone target of Sirt1. Etoposide treatment significantly decreased Bax mRNA levels in TPC1 cells (Fig. 10A), whereas it remarkably upregulated Bax expression in FRO cells (Fig. 10C). Bcl-xL

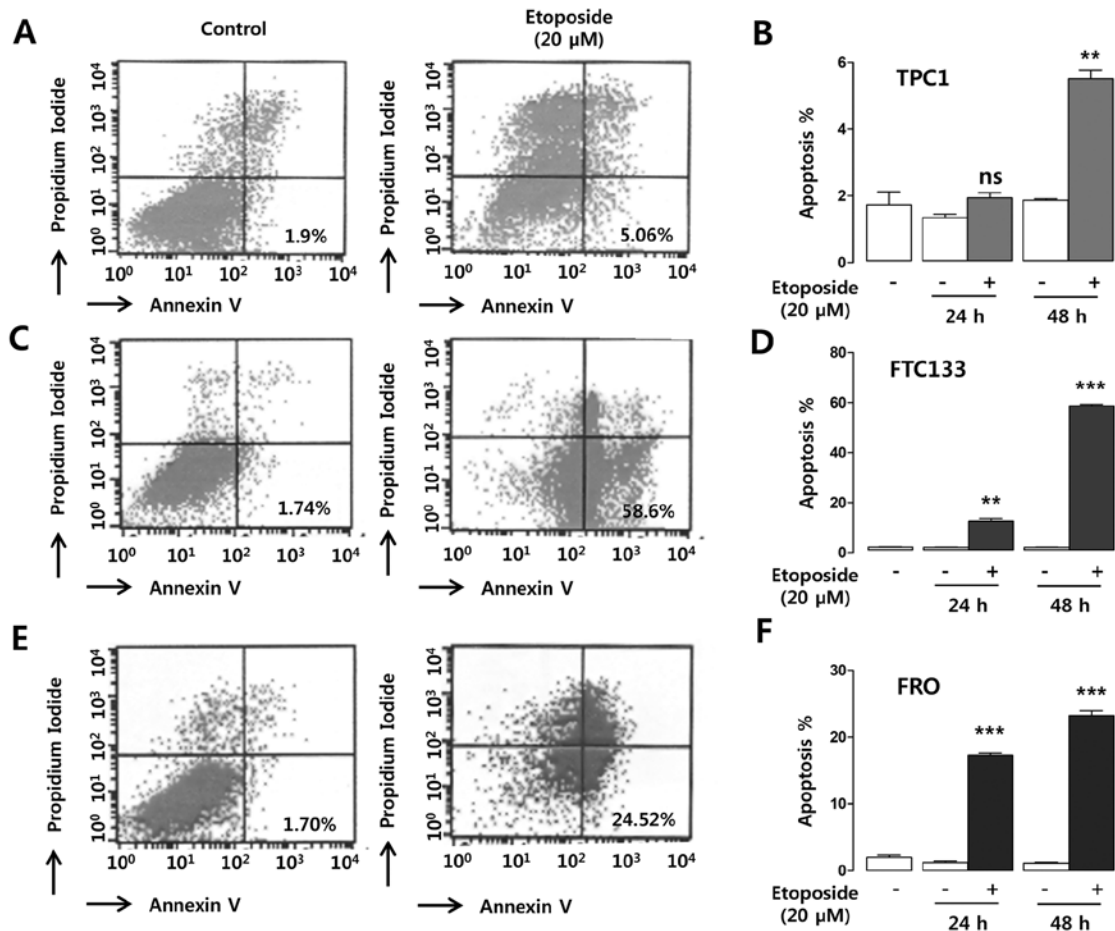


Figure 7. Representative results of Annexin V flow cytometry and quantitative analysis of early apoptotic cells (negative propidium iodide and positive Annexin V staining cells) with or without etoposide treatment for the indicated times in TPC1 (A and B), FTC133 (C and D) and FRO (E and F) cells. (A, C and E) Representative flow cytometry results in cells treated with etoposide (20 μM) for 48 h. The data are the result of three independent experiments, each performed in triplicate. Comparisons were performed using the Mann-Whitney U test. Data are expressed as mean ± SEM, **p<0.01, ***p<0.001. All reported p-values are two-sided.

and p53 showed decreased mRNA expression in the three cell lines after etoposide treatment (Fig. 10A-C). p21 expression was significantly upregulated in TPC1 cells and downregulated in FRO cells, suggesting a cytoprotective effect for p21 in TPC1 cells (Fig. 10A, C and D). The downregulation of Bax and upregulation of p21 in TPC1 cells suggests that the higher induction of Sirt1 confers increased resistance to etoposide-induced apoptosis via Sirt1-Foxp3-Bax/p21 signaling.

Discussion

The use of selective RAF/MEK small molecule kinase inhibitors as monotherapy has been examined in clinical trials (28,29). The US Food and Drug Administration expanded the approved uses of Nexavar (Sorafenib)[®] to the treatment of late-stage (metastatic) DTC. However, the development of resistance against RAF inhibitors is an emerging obstacle to the treatment of RAI-refractory thyroid cancers (9,30) and the development of novel therapeutic drugs. To overcome these limitations, significant efforts have been directed to improving our understanding of the mechanisms underlying thyroid carcinogenesis. For example, protein interactions between RAF paralogs have been suggested as a possible drug resis-

tance mechanism (31-33). Point mutations in RAS or MEK are known to generate MEK/ERK signal propagation in response to selective RAF kinase inhibitors (34). Mitogen-activated protein kinase kinase kinase 8 [MAP3K8, cancer Osaka thyroid (COT)] overexpression is another proposed mechanism of drug resistance (35). Ligand-specific receptor tyrosine kinase activation is a druggable target in RAI-refractory thyroid cancers (36-38). Recently, MEK-ERK independent signaling pathways involved in thyroid carcinogenesis have been investigated (39-42).

The sirtuin family, which includes seven members (SIRT1-SIRT7), has emerged as an important regulator of diverse physiologic or pathologic events including life-span extension, age-related disorders and cancer (19). However, studies have suggested that Sirt1 can act as either a tumor suppressor or promoter depending on its targets in specific signaling pathways or in specific cancers, and its role therefore remains unclear (24,25).

In the present study, we first investigated whether Sirt1 expression could be used as a molecular marker to differentiate thyroid cancers from normal thyroid cells. Unfortunately, the IHC data showed heterogenous expression of Sirt1 and Sirt3, which prevented us using the expression of these proteins to

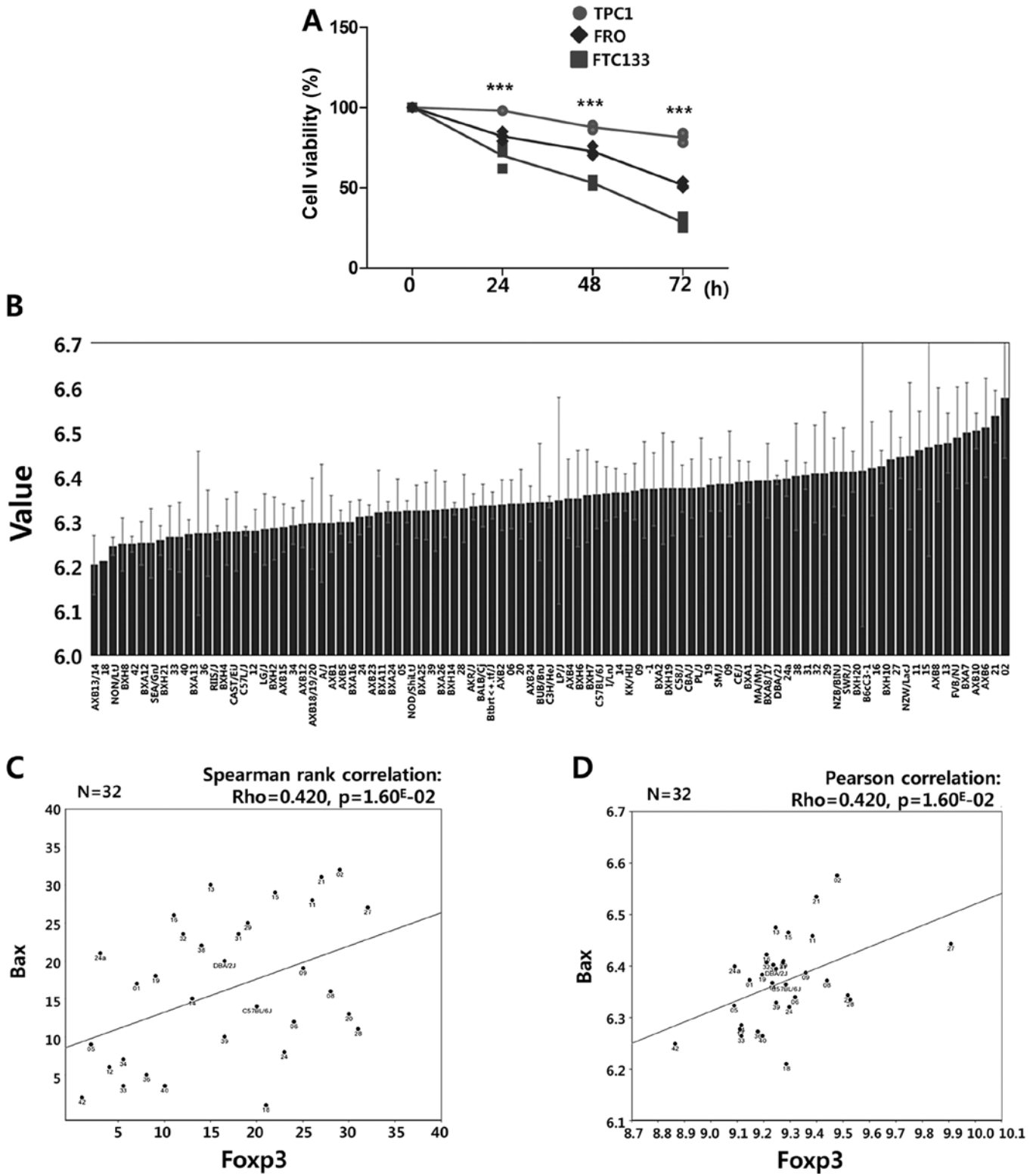


Figure 8. MTT assay and correlation analysis between Foxp3 and Bax in the GSE16780 UCLA Hybrid MDP Liver Affy HT M430A (Sep11) RMA Database using GeneNetwork (<http://www.genenetwork.org/>). (A) MTT assay to observe cell viability in response to etoposide treatment for the indicated times. Comparisons were performed using the Mann-Whitney U test. Data are expressed as each replicate, * $p < 0.05$, ** $p < 0.01$, *** $p < 0.001$. All reported p-values are two-sided. (B-D) Correlation analysis between Bax and Foxp3. Ranked bar graph showing the number of samples and Foxp3 expression values in each mouse (B). Spearman's rank correlation: $Rho = 0.420, p = 1.60 \times 10^{-2}$ (C). Pearson's correlation: $Rho = 0.453, p = 8.49 \times 10^{-3}$ (D).

discriminate between cancer cells and normal cells. Data from the Human Protein Atlas (HPA), a scientific research program that aims to explore the whole human proteome using an

antibody-based approach, showed heterogeneous expression of Sirt1 and Sirt3 in normal follicular cells and papillary thyroid cancer cells (43). Consistently, BioGPS and NCBI Gene

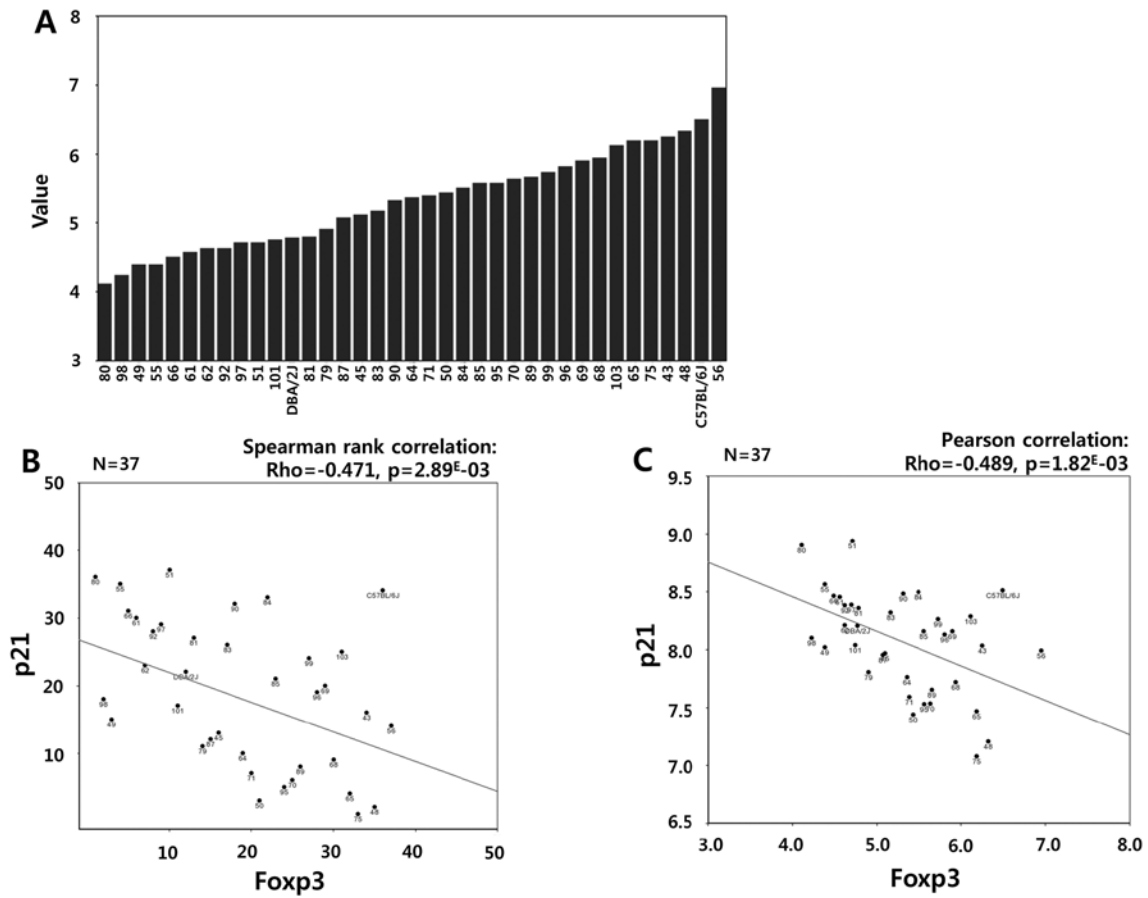


Figure 9. Correlation analysis between Foxp3 and P21 in EPFL/LISP BXD CD Brown Adipose Affy Mouse Gene 2.0 ST Exon Level (Oct13) RMA using GeneNetwork (<http://www.genenetwork.org/>). (A) Ranked bar graph showing the number of samples and p21 expression values in each individual mouse. (B) Spearman's rank correlation: $Rho=-0.471$, $p=2.89E-03$. (C) Pearson's correlation: $Rho=-0.489$, $p=1.82E-03$.

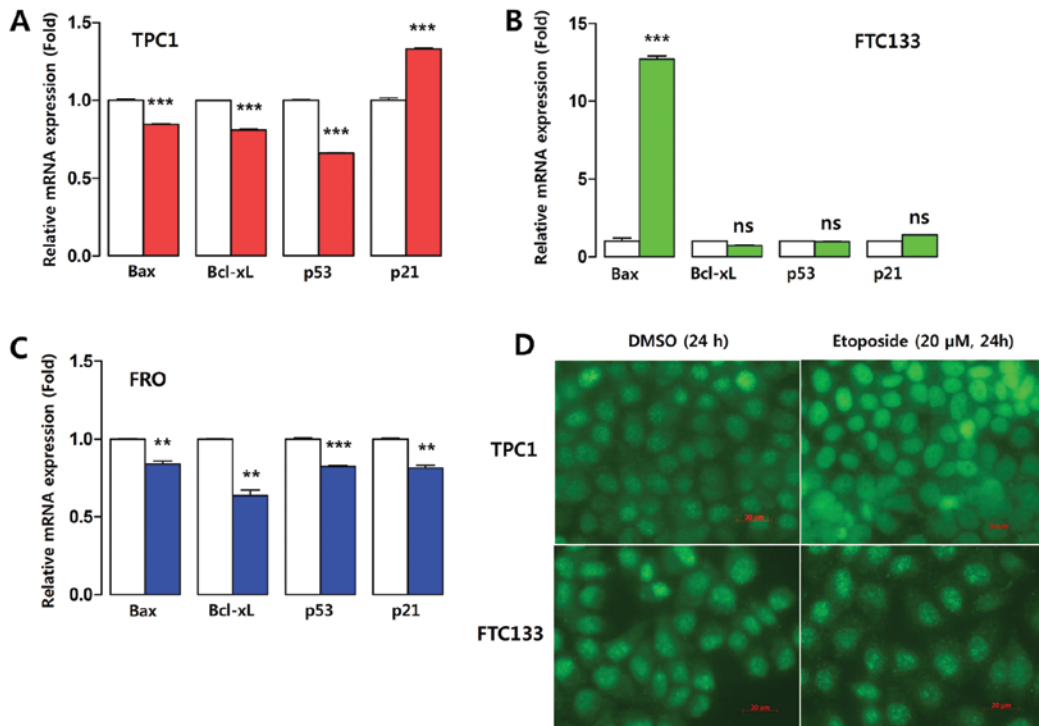


Figure 10. mRNA expression of Bax, Bcl-X1, p53 and p21 in response to etoposide treatment for 48 h was assessed by qRT-PCR in TPC1 (A), FTC133 (B) and FRO (C) cells. qRT-PCR experiments were performed in triplicate and repeated three times. Comparisons were performed using the Mann-Whitney U test. Data are expressed as mean \pm SEM; ** $p<0.01$, *** $p<0.001$. All reported p-values are two-sided. (D) Representative figures of immunofluorescence staining for p21 in TPC1 and FTC133 cells with or without etoposide treatment. Data are the representative result of three independent experiments.

Expression Omnibus (GEO) profiles also indicated heterogeneous expression of Sirt1 and Sirt3 in normal follicular cells and papillary thyroid cancer cells, as well as breast cancer cell lines. Additionally, western blot analysis indicated variable baseline Sirt1 and Sirt3 protein levels in TPC1 (papillary), FTC133 (follicular) and FRO (anaplastic) cells (data not shown). The cell type-dependent differential induction of Sirt1 and Sirt3 expression by etoposide suggested that Sirt1 and Sirt3 induction in thyroid cancer cell lines is related to the response to drug-induced genotoxic stress. Consistent with this hypothesis, TPC1 cells, which have the highest induction of the three cell lines, were more resistant to etoposide treatment than FTC133 and FRO cells, as demonstrated by Annexin V apoptosis and MTT assays.

To identify the signaling pathway mediating the resistance to drug-induced genotoxic stress, we performed qRT-PCR for Bcl2 family proteins such as pro-apoptotic Bax and anti-apoptotic Bcl-xL. The expression of p21, a cyclin-dependent kinase inhibitor that is induced by p53-dependent and -independent mechanisms in response to stress, was also assessed by qRT-PCR (44). Our results showed that etoposide downregulated pro-apoptotic Bcl2 family proteins and p53 and upregulated p21 expression in TPC1 cells. Previous studies suggested that p21 suppresses tumor development by inhibiting cell cycle progression in response to various stimuli. Additionally, several biochemical and genetic studies have indicated that p21 acts as a master effector of multiple tumor suppressor pathways that are independent of the classical p53 pathway (44). Despite its known anti-proliferative role and its ability to promote cellular senescence, recent studies have suggested that, under certain conditions, p21 can promote cellular proliferation and oncogenicity (45). Consequently, p21 is often dysregulated in human cancers, although it has been shown to act as a tumor suppressor or oncogene depending on the cellular context and conditions (45,46). Recent studies also suggested that p21 suppresses the induction of pro-apoptotic genes by MYC and E2F1 through direct binding and inhibition of their transactivation functions (47). In addition, p21 plays an important role in modulating DNA repair processes by inhibiting cell cycle progression and allowing DNA repair to proceed while inhibiting apoptosis. Furthermore, p21 can compete for PCNA binding with several PCNA-reliant proteins involved directly in DNA repair processes (48).

To the best of our knowledge, a direct relationship between Sirt1 and Bax or p21 independently from the p53 pathway has not been investigated to date. However, Foxp3, which is deacetylated and degraded by Sirt1, showed a statistically significant strong positive correlation with Bax and negative correlation with p21 in our analysis using GeneNetwork. These results suggested that a Sirt1-Foxp3 signaling axis may be a signature molecular event in TPC1 cells associated with resistance against etoposide-induced genotoxic stress (49).

In conclusion, we showed that Sirt1 and Sirt3 are expressed at different levels in different cell and tissue samples. Furthermore, the induction of Sirt1 and Sirt3 expression differed among thyroid cancer cell lines and was correlated with survival under conditions of genotoxic stress. Our results suggest the involvement of a Sirt1-Foxp3 signaling pathway in the resistance of thyroid cancer cells against genotoxic stress. The role of p21 in cells exposed to genotoxic stress should be

addressed in future studies to identify novel therapeutic targets for the treatment of RAI-refractory thyroid cancer.

Acknowledgements

This study was supported by a faculty research grant of Yonsei University College of Medicine (6-2014-0056).

References

- Lang BH, Wong KP, Cheung CY, Wan KY and Lo CY: Evaluating the prognostic factors associated with cancer-specific survival of differentiated thyroid carcinoma presenting with distant metastasis. *Ann Surg Oncol* 20: 1329-1335, 2013.
- Lin JD, Huang MJ, Juang JH, *et al*: Factors related to the survival of papillary and follicular thyroid carcinoma patients with distant metastases. *Thyroid* 9: 1227-1235, 1999.
- Sabra MM, Dominguez JM, Grewal RK, *et al*: Clinical outcomes and molecular profile of differentiated thyroid cancers with radioiodine-avid distant metastases. *J Clin Endocrinol Metab* 98: E829-E836, 2013.
- Droz JP, Schlumberger M, Rougier P, Ghosn M, Gardet P and Parmentier C: Chemotherapy in metastatic nonanaplastic thyroid cancer: experience at the Institut Gustave-Roussy. *Tumori* 76: 480-483, 1990.
- Schlumberger M: Target therapies for radioiodine refractory advanced thyroid tumors. *J Endocrinol Invest* 35: 40-44, 2012.
- Salvatore G, De Falco V, Salerno P, *et al*: BRAF is a therapeutic target in aggressive thyroid carcinoma. *Clin Cancer Res* 12: 1623-1629, 2006.
- Xing M: BRAF mutation in papillary thyroid cancer: pathogenic role, molecular bases, and clinical implications. *Endocr Rev* 28: 742-762, 2007.
- Liu D, Hu S, Hou P, Jiang D, Condouris S and Xing M: Suppression of BRAF/MEK/MAP kinase pathway restores expression of iodide-metabolizing genes in thyroid cells expressing the V600E BRAF mutant. *Clin Cancer Res* 13: 1341-1349, 2007.
- Lito P, Rosen N and Solit DB: Tumor adaptation and resistance to RAF inhibitors. *Nat Med* 19: 1401-1409, 2013.
- Montero-Conde C, Ruiz-Llorente S, Dominguez JM, *et al*: Relief of feedback inhibition of HER3 transcription by RAF and MEK inhibitors attenuates their antitumor effects in BRAF-mutant thyroid carcinomas. *Cancer Discov* 3: 520-533, 2013.
- Haigis MC and Guarente LP: Mammalian sirtuins - emerging roles in physiology, aging, and calorie restriction. *Genes Dev* 20: 2913-2921, 2006.
- Luo J, Nikolaev AY, Imai S, *et al*: Negative control of p53 by Sir2alpha promotes cell survival under stress. *Cell* 107: 137-148, 2001.
- Westerheide SD, Anckar J, Stevens SM Jr, Sistonen L and Morimoto RI: Stress-inducible regulation of heat shock factor 1 by the deacetylase SIRT1. *Science* 323: 1063-1066, 2009.
- Rodgers JT, Lerin C, Haas W, Gygi SP, Spiegelman BM and Puigserver P: Nutrient control of glucose homeostasis through a complex of PGC-1alpha and SIRT1. *Nature* 434: 113-118, 2005.
- Rodgers JT, Lerin C, Gerhart-Hines Z and Puigserver P: Metabolic adaptations through the PGC-1 alpha and SIRT1 pathways. *FEBS Lett* 582: 46-53, 2008.
- Brunet A, Sweeney LB, Sturgill JF, *et al*: Stress-dependent regulation of FOXO transcription factors by the SIRT1 deacetylase. *Science* 303: 2011-2015, 2004.
- Brachmann CB, Sherman JM, Devine SE, Cameron EE, Pillus L and Boeke JD: The SIR2 gene family, conserved from bacteria to humans, functions in silencing, cell cycle progression, and chromosome stability. *Genes Dev* 9: 2888-2902, 1995.
- Bishop NA and Guarente L: Genetic links between diet and lifespan: shared mechanisms from yeast to humans. *Nat Rev Genet* 8: 835-844, 2007.
- Raynes R, Brunquell J and Westerheide SD: Stress inducibility of SIRT1 and its role in cytoprotection and cancer. *Genes Cancer* 4: 172-182, 2013.
- Verdin E: AROUSING SIRT1: identification of a novel endogenous SIRT1 activator. *Mol Cell* 28: 354-356, 2007.
- Gorospe M and de Cabo R: ASIRTING the DNA damage response. *Trends Cell Biol* 18: 77-83, 2008.

22. Brennan CM and Steitz JA: HuR and mRNA stability. *Cell Mol Life Sci* 58: 266-277, 2001.
23. Lopez de Silanes I, Zhan M, Lal A, Yang X and Gorospe M: Identification of a target RNA motif for RNA-binding protein HuR. *Proc Natl Acad Sci USA* 101: 2987-2992, 2004.
24. Song NY and Surh YJ: Janus-faced role of SIRT1 in tumorigenesis. *Ann NY Acad Sci* 1271: 10-19, 2012.
25. Bosch-Presegue L and Vaquero A: The dual role of sirtuins in cancer. *Genes Cancer* 2: 648-662, 2011.
26. Yuan J, Luo K, Liu T and Lou Z: Regulation of SIRT1 activity by genotoxic stress. *Genes Dev* 26: 791-796, 2012.
27. Kwon HS, Lim HW, Wu J, Schnolzer M, Verdin E and Ott M: Three novel acetylation sites in the Foxp3 transcription factor regulate the suppressive activity of regulatory T cells. *J Immunol* 188: 2712-2721, 2012.
28. Bollag G, Tsai J, Zhang J, *et al*: Vemurafenib: the first drug approved for BRAF-mutant cancer. *Nat Rev Drug Discov* 11: 873-886, 2012.
29. Turajlic S, Ali Z, Yousaf N and Larkin J: Phase I/II RAF kinase inhibitors in cancer therapy. *Expert Opin Investig Drugs* 22: 739-749, 2013.
30. Brilli L and Pacini F: Targeted therapy in refractory thyroid cancer: current achievements and limitations. *Future Oncol* 7: 657-668, 2011.
31. Poulidakos PI, Zhang C, Bollag G, Shokat KM and Rosen N: RAF inhibitors transactivate RAF dimers and ERK signalling in cells with wild-type BRAF. *Nature* 464: 427-430, 2010.
32. Poulidakos PI, Persaud Y, Janakiraman M, *et al*: RAF inhibitor resistance is mediated by dimerization of aberrantly spliced BRAF(V600E). *Nature* 480: 387-390, 2011.
33. Montagut C, Sharma SV, Shioda T, *et al*: Elevated CRAF as a potential mechanism of acquired resistance to BRAF inhibition in melanoma. *Cancer Res* 68: 4853-4861, 2008.
34. Greger JG, Eastman SD, Zhang V, *et al*: Combinations of BRAF, MEK, and PI3K/mTOR inhibitors overcome acquired resistance to the BRAF inhibitor GSK2118436 dabrafenib, mediated by NRAS or MEK mutations. *Mol Cancer Ther* 11: 909-920, 2012.
35. Johannessen CM, Boehm JS, Kim SY, *et al*: COT drives resistance to RAF inhibition through MAP kinase pathway reactivation. *Nature* 468: 968-972, 2010.
36. Su F, Bradley WD, Wang Q, *et al*: Resistance to selective BRAF inhibition can be mediated by modest upstream pathway activation. *Cancer Res* 72: 969-978, 2012.
37. Nazarian R, Shi H, Wang Q, *et al*: Melanomas acquire resistance to B-RAF(V600E) inhibition by RTK or N-RAS upregulation. *Nature* 468: 973-977, 2010.
38. Atefi M, von Euw E, Attar N, *et al*: Reversing melanoma cross-resistance to BRAF and MEK inhibitors by co-targeting the AKT/mTOR pathway. *PLoS One* 6: e28973, 2011.
39. Sanchez-Hernandez I, Baquero P, Calleros L and Chilocheas A: Dual inhibition of (V600E)BRAF and the PI3K/AKT/mTOR pathway cooperates to induce apoptosis in melanoma cells through a MEK-independent mechanism. *Cancer Lett* 314: 244-255, 2012.
40. Vergani E, Vallacchi V, Frigerio S, *et al*: Identification of MET and SRC activation in melanoma cell lines showing primary resistance to PLX4032. *Neoplasia* 13: 1132-1142, 2011.
41. Lee MH, Lee SE, Kim DW, *et al*: Mitochondrial localization and regulation of BRAFV600E in thyroid cancer: a clinically used RAF inhibitor is unable to block the mitochondrial activities of BRAFV600E. *J Clin Endocrinol Metab* 96: E19-E30, 2011.
42. Lee SE, Lee JU, Lee MH, *et al*: RAF kinase inhibitor-independent constitutive activation of Yes-associated protein 1 promotes tumor progression in thyroid cancer. *Oncogenesis* 2: e55, 2013.
43. Uhlen M, Oksvold P, Fagerberg L, *et al*: Towards a knowledge-based Human Protein Atlas. *Nat Biotechnol* 28: 1248-1250, 2010.
44. Zuo S, Liu C, Wang J, *et al*: IGFBP-rP1 induces p21 expression through a p53-independent pathway, leading to cellular senescence of MCF-7 breast cancer cells. *J Cancer Res Clin Oncol* 138: 1045-1055, 2012.
45. Warfel NA and El-Deiry WS: p21^{WAF1} and tumourigenesis: 20 years after. *Curr Opin Oncol* 25: 52-58, 2013.
46. Deng C, Zhang P, Harper JW, Elledge SJ and Leder P: Mice lacking p21^{CIP1/WAF1} undergo normal development, but are defective in G1 checkpoint control. *Cell* 82: 675-684, 1995.
47. Gartel AL and Tyner AL: Transcriptional regulation of the p21((WAF1/CIP1)) gene. *Exp Cell Res* 246: 280-289, 1999.
48. Abbas T and Dutta A: p21 in cancer: intricate networks and multiple activities. *Nat Rev Cancer* 9: 400-414, 2009.
49. van Loosdregt J, Brunen D, Fleskens V, Pals CE, Lam EW and Coffey PJ: Rapid temporal control of Foxp3 protein degradation by sirtuin-1. *PLoS One* 6: e19047, 2011.